Supplementary Material for

Flow-regime-controlled mass transfer intensification for fabricating superior silicon-carbon anode materials

Fan Liu [a,b,*], Hebang Shi [b,*], Yuqi Geng [b], Hongtao Li [b,c,*], Qigao Cao [a]

a) Institute of Electronic Materials, Northwest Institute for Non-ferrous Metal Research, Xi'an 710016, China

b) State Key Laboratory of Mesoscience and Engineering, Institute of Process Engineering, Chinese Academy of Sciences, Beijing 100190, China

c) Henan Key Laboratory of Advanced Conductor Materials, Institute of Materials, Henan Academy of Sciences, Zhengzhou 450001, China

*Correspondence author:

Fan Liu;

E-mail: liufan191@mails.ucas.ac.cn;

Tel./Fax: +86-18612909994.

Hebang Shi;

E-mail: hbshi@ipe.ac.cn;

Hongtao Li;

E-mail: lihongtao@hnas.ac.cn;

1. Evolution of agglomerate sizes

As shown in Fig. S1, the fluidized pressure drop of the powder always approaches the theoretical value in the particulate fluidization regime, indicating that the powder is fully fluidized. Without stirring, the pressure drop is much lower than the theoretical value and almost zero, indicating that the powder has not undergone fluidization. Furthermore, our stability analysis of the particulate fluidization regime reveals that once established, the bed maintains a stable and homogeneous fluidized state throughout the operation. This behavior, marked by consistent pressure drop and uniform expansion, stands in sharp contrast to the inherently unstable and heterogeneous nature of traditional bubbling fluidization.

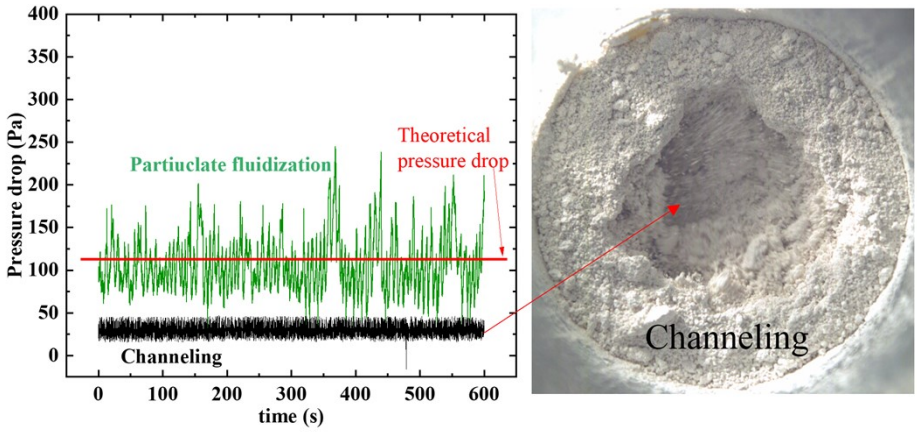

Fig. S1. Pressure drop under particulate fluidization and channeling

Fig. S2 presents optical micrographs of agglomerates at different stirring speeds. Due to their large size, which often precludes viable SEM sample preparation, agglomerates were directly examined via microscopy. At low speeds, millimeter-sized agglomerates were observed. Conversely, increasing the stirring speed led to a pronounced reduction in agglomerate size. Ultimately, at the rotational speed required for particulate fluidization, the agglomerate size was reduced to below 100 μm.

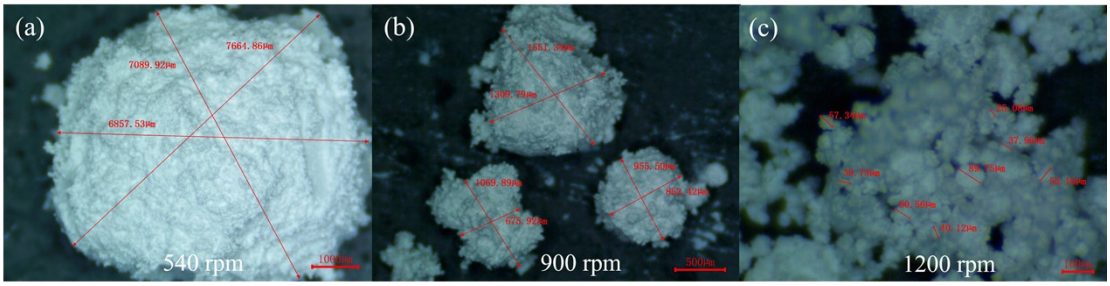

Fig. S2. Picture of agglomerates during fluidization under (a) 540 rpm, (b) 900 rpm and (c) 1200 rpm

As shown in Fig. S3a, all these values of stirring speed could make the TiO_2 powders fluidize in the regime of particulate fluidization regime. All these breakthrough curves were similar to one another especially at the initial stage of adsorption, indicating that the breakthrough time in the particulate fluidization regime was hardly affected by stirring speed. As a result, if the particles fluidized in the particulate fluidization regime, the gas-solid contact performance could be the best among all the regimes under the assistance of stirring.

Nonetheless, the stirring speed still had an influence on the total amount of adsorbed gas in the particulate fluidization. For one thing, the turbulence degree of gas-solid fluidization increased with the increase of stirring speed. According to the standard deviation of pressure drop fluctuation (Fig. S3b), increasing stirring speed inhibited bubbles and reduced pressure fluctuation during the transition from bubbling to particulate fluidization. However, the pressure pulsation was increased with the stirring speed when the powder was in the regime of particulate fluidization, which may also be the reason for a small decrease in mass transfer at high stirring speed. Another thing is that increasing the stirring speed would increase the flow velocity of the gas phase, resulting in a lower residence time of the gas in the bed, and thus may also reduce the total amount of adsorption.

Therefore, besides managing the operational mode and transitions in the regime, it is also essential to operate at low stirring speeds whenever the particulate fluidization is stable, as this can further enhance mass transfer efficiency. Moreover, from an energy standpoint, a lower stirring speed translates to reduced energy consumption. This stable, low-speed operation is also conducive to scaling up processes with reduced energy use

and improved economic efficiency.

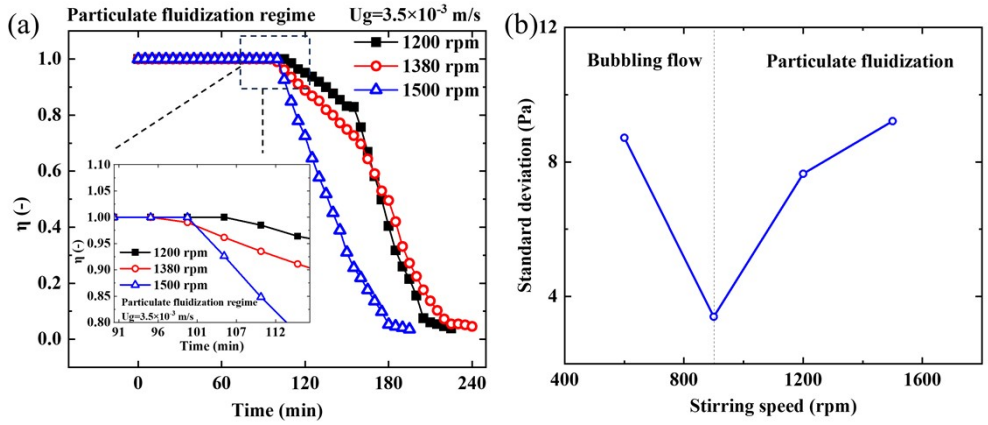

Fig. S3. Effect of stirring speed on breakthrough curves in particulate fluidization regime.

CV curves (Fig. S4a) indicate that as the fluidization quality deteriorates, the peak current of the samples gradually decreases, implying a reduction in their electrochemical activity. Among them, PF-Si@Cexhibits the highest electrochemical activity. EIS (Fig. S4b) results show that after cycling, PF-Si@C exhibits the smallest increase in charge-transfer resistance (Rct), indicating an intact carbon coating layer, a stable Si/C interface, and a more efficient electron transport pathway. BF-Si@C shows a moderate increase in Rct, whereas CP-Si@C and CH-Si@C display a significant rise in Rct. This reveals severe interfacial side reactions and contact failure caused by uneven coating or poor contact. The initial charge–discharge curves (Fig. S4c) demonstrate that PF-Si@C achieves the highest initial Coulombic efficiency, while the efficiencies of samples from the other three fluidization regimes are lower, especially for CP-Si@C and CH-Si@C. Furthermore, deteriorating fluidization quality leads to a gradual decrease in the minimum lithiation potential, thereby increasing the energy barrier for lithium intercalation. Rate capability tests (Fig.S4d) reveal that the overall rate performance of PF-Si@C is superior to that of samples from other fluidization

regimes. This indicates that the coating quality under this optimal regime is the best, effectively accommodating the expansion and contraction of silicon. The primary reasons are: the uniform distribution of solid carbon on the C-Si surface and within its pores enhances electronic conductivity; the coated carbon layer on the C-Si surface mitigates stress concentration and structural damage during silicon volume expansion; and it isolates direct contact between the C-Si surface and the electrolyte, reducing the likelihood of side reactions.

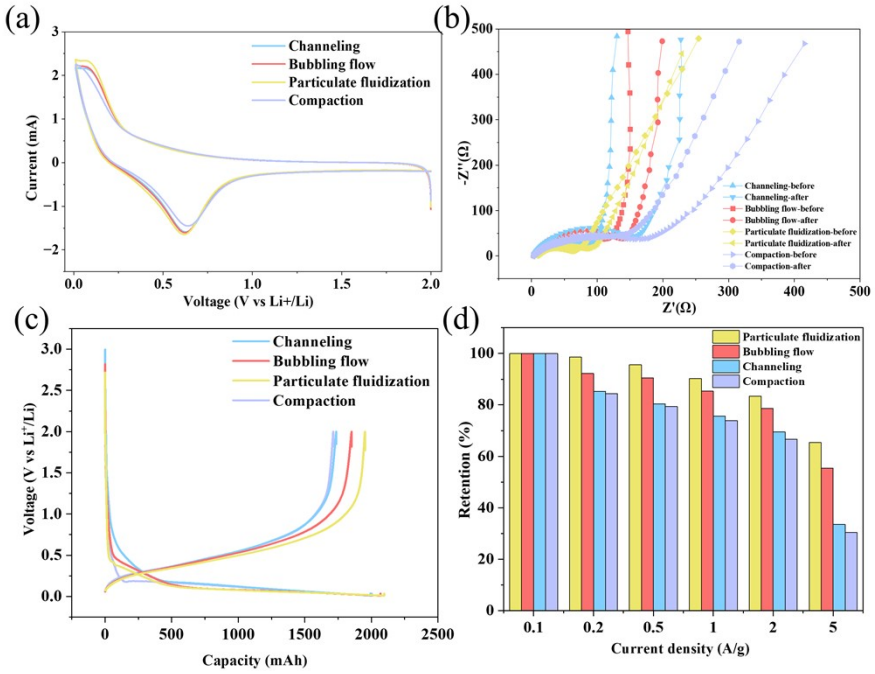

Fig. S4. Comparative electrochemical performance under different flow regimes. (a) CV curves. (b) EIS spectra (initial and after cycling). (c) Charge-discharge profiles. (d) Rate capability at varying current densities..

2. Agglomerate size characterization

The agglomerate size was determined following a previously established protocol [36]. Samples were collected at 540, 900, and 1200 rpm by slowly decreasing the gas velocity after 30 minutes of fluidization, allowing the agglomerates to exit smoothly via the sampling hole. The morphology of the large agglomerates was then examined using a stereomicroscope (XTZ-T, Beijing Boyuan Xiangde Scientific Instrument Co.,

Ltd, China). The equivalent diameter of stable agglomerates was quantified by averaging the lengths of three lines passing through their center, a method applied regardless of their sphericity. Finally, the size distribution was analyzed with Nano Measurer software.